

1 Nitrogen Fixation in Arctic Coastal Waters (Qeqertarsuaq, West 2 Greenland): Influence of Glacial Melt on Diazotrophs, Nutrient 3 Availability, and Seasonal Blooms

4 Schlangen Isabell¹, Leon-Palmero Elizabeth^{1,2}, Moser Annabell¹, Xu Peihang¹, Laursen Erik¹, and
5 Löscher Carolin R.^{1,3}

6 ¹Nordceee, Department of Biology, University of Southern Denmark, Campusvej 55, 5230 Odense M, Denmark

7 ²Department of Geosciences, Princeton University, Princeton, New Jersey

8 ³DIAS, University of Southern Denmark, Odense, Denmark

9 **Correspondence:** Carolin R. Löscher (cloescher@biology.sdu.dk)

10
11 **Abstract.** The Arctic Ocean is undergoing rapid transformation due to climate change, with decreasing sea ice contributing to
12 a predicted increase in primary productivity. A critical factor determining future productivity in this region is the availability
13 of nitrogen, a key nutrient that often limits biological growth in Arctic waters. The fixation of dinitrogen (N₂) gas, a biological
14 process mediated by diazotrophs, not only supplies new nitrogen to the ecosystem but also plays a central role in shaping
15 the biological productivity of the Arctic. Historically it was believed to be limited to oligotrophic tropical and subtropical
16 oceans, Arctic N₂ fixation has only garnered significant attention over the past decade, leaving a gap in our understanding
17 of its magnitude, the diazotrophic community, and potential environmental drivers. In this study, we investigated N₂ fixation
18 rates and the diazotrophic community in Arctic coastal waters, using a combination of isotope labeling, genetic analyses and
19 biogeochemical profiling, in order to explore its response to glacial meltwater, nutrient availability and its impact on primary
20 productivity. Here we show N₂ fixation rates ranging from 0.16 to 2.71 nmol N L⁻¹ d⁻¹, to be notably higher than those observed
21 in many other oceanic regions, suggesting a previously unrecognized significance of N₂ fixation in these high-latitude waters.
22 The diazotrophic community is predominantly composed of UCYN-A. We found highest N₂ fixation rates co-occurring with
23 maximum chlorophyll *a* concentrations and primary production rates at a station in the Vaigat Strait close impacted by glacier
24 meltwater inflow, possibly providing otherwise limiting nutrients. Our findings illustrate the importance of N₂ fixation in an
25 environment previously not considered important for this process and provide insights into its response to the projected melting
26 of the polar ice cover.

27 28 1 Introduction

29
30 Nitrogen is a key element for life and often acts as a growth-limiting factor for primary productivity (Gruber and Sarmiento,
31 1997; Gruber, 2004; Gruber and Galloway, 2008). Despite nitrogen gas (N₂) making up approximately 78% of the atmosphere,
32 it remains inaccessible to most marine life forms. Diazotrophs, which are specialized bacteria and archaea, have the ability to
33 convert N₂ into biologically available nitrogen, facilitated by the nitrogenase enzyme complex carrying out the process of
34 biological nitrogen fixation (N₂ fixation) (Capone and Carpenter (1982)). Despite the fact that these organisms are highly spe-

35 cialized and N₂ fixation is energetically demanding, the ability to carry out this process is widespread amongst prokaryotes.
36 However, it is controlled by several factors such as temperature, light, nutrients and trace metals such as iron and molybdenum
37 (Sohm et al., 2011; Tang et al., 2019). Oceanic N₂ fixation is the major source of nitrogen to the marine system (Karl et al.,
38 2002; Gruber and Sarmiento, 1997), thus, diazotrophs determine the biological productivity of our planet (Falkowski et al.
39 (2008), impact the global carbon cycle and the formation of organic matter (Galloway et al., 2004; Zehr and Capone, 2020).
40 Traditionally it has been believed that the distribution of diazotrophs was limited to warm and oligotrophic waters (Buchanan
41 et al., 2019; Sohm et al., 2011; Luo et al., 2012) until putative diazotrophs were identified in the central Arctic Ocean and
42 Baffin Bay (Farnelid et al., 2011; Damm et al., 2010). First rate measurements have been reported for the Canadian Arctic by
43 Blais et al. (2012) and recent studies have reported rate measurements in adjacent seas (Harding et al., 2018; Sipler et al., 2017;
44 Shiozaki et al., 2017, 2018), drawing attention to cold and temperate waters as significant contributors to the global nitrogen
45 budget through diverse organisms.

46 N₂ fixation is performed by diverse group of cyanobacteria as well as by non-cyanobacteria diazotrophs (NCDs). UCYN-A
47 has been described as the dominant active N₂ fixing cyanobacterial diazotroph in arctic waters (Harding et al. (2018)), while
48 other cyanobacteria have only occasionally been reported (Díez et al., 2012; Fernández-Méndez et al., 2016; Blais et al., 2012).
49 Recent studies found that the majority of the arctic marine diazotrophs are NCDs and those may contribute significantly to N₂
50 fixation in the Arctic Ocean (Shiozaki et al., 2018; Fernández-Méndez et al., 2016; Harding et al., 2018; Von Friesen and Rie-
51 mann, 2020). Still, studies on the Arctic diazotroph community remain scarce, leaving Arctic environments poorly understood
52 regarding N₂ fixation. Shao et al. (2023) note the impossibility of estimating Arctic N₂ fixation rates due to the sparse spatial
53 coverage, which currently represents only approximately 1 % of the Arctic Ocean. Increasing data coverage in future studies
54 will aid in better constraining the contribution of N₂ fixation to the global oceanic nitrogen budget (Tang et al. (2019)).

55 The Arctic ecosystem is undergoing significant changes driven by rising temperatures and the accelerated melting of sea ice, a
56 trend predicted to intensify in the future (Arrigo et al., 2008; Hanna et al., 2008; Haine et al., 2015). These climate-driven shifts
57 have stimulated primary productivity in the Arctic by 57 % from 1998 to 2018, elevating nutrient demands in the Arctic Ocean
58 (Ardyna and Arrigo, 2020; Arrigo and van Dijken, 2015; Lewis et al., 2020). This increase is attributed to prolonged
59 phytoplankton growing seasons and expanding ice-free areas suitable for phytoplankton growth (Arrigo et al. (2008)).
60 However, despite these dramatic changes, the role of N₂ fixation in sustaining Arctic primary production remains poorly
61 understood. While recent studies suggest that diazotrophic activity may contribute to nitrogen inputs in polar regions (Sipler
62 et al. (2017)), fundamental uncertainties remain regarding the extend, distribution and environmental drivers of N₂ Fixation in
63 the Arctic Ocean. Specifically, it is unclear whether increased glacial meltwater input enhances or inhibits N₂ Fixation through
64 changes in nutrient availability, stratification, and microbial community composition. Thus, the question of whether nitrogen
65 limitation will emerge as a key factor constraining Arctic primary production under future climate scenarios remains unresolved. In this
66 study, we investigate the diversity of diazotrophic communities alongside in situ N₂ fixation rate measurements in Disko Bay
67 (Qeqertarsuaq), a coastal Arctic system strongly influenced by glacial meltwater input. By linking environmental parameters to N₂
68 fixation dynamics, we aim to clarify the role of diazotrophs in Arctic nutrient cycling and assess their potential contribution to

69 sustaining primary production in a changing Arctic. Understanding these processes is essential for refining biogeochemical
70 models and predicting ecosystem responses to future climate change.

71

72 **2 Material and methods**

73

74 **2.1 Seawater sampling**

75

76 The research expedition was conducted from August 16 to 26 in 2022 aboard the Danish military vessel P540 within the waters
77 of Qeqertarsuaq, located in the western region of Greenland (Kalaallit Nunaat). Discrete water samples were obtained using a
78 10 L Niskin bottle, manually lowered with a hand winch to five distinct depths (surface, 5, 25, 50, and 100 m). A comprehensive
79 sampling strategy was employed at 10 stations (Fig. 1), covering the surface to a depth of 100 m. The sampled parameters
80 included water characteristics, such as nutrient concentrations, chl *a*, particulate organic carbon (POC) and nitrogen (PON),
81 molecular samples for nucleic acid extractions (DNA), dissolved inorganic carbon (DIC) as well as CTD sensor data. At three
82 selected stations (3,7,10) N₂ fixation and primary production rates were quantified through concurrent incubation experiments.
83 Samples for nutrient analysis, nitrate (NO₃⁻), nitrite (NO₂⁻) and phosphate (PO₄³⁻) were taken in triplicates, filtered through
84 a 0.22 μ m syringe filter (Avantor VWR® Radnor, Pa, USA) and stored at -20 °C until further analysis. Concentrations were
85 spectrophotometrically determined (Thermo Scientific, Genesys 1OS UV-VIS spectrophotometer) following the established
86 protocols of Murphy and Riley (1962) for PO₄³⁻; García-Robledo et al. (2014) for NO₃⁻ & NO₂⁻ (detection limits: 0.01 μ mol
87 L⁻¹ (NO₃⁻, NO₂⁻, and PO₄³⁻), 0.05 μ mol L⁻¹ (NH₄⁺)). Chl *a* samples were filtered onto 47 mm ø GF/F filters (GE Healthcare
88 Life Sciences, Whatman, USA), placed into darkened 15 mL LightSafe centrifuge tubes (Merck, Rahway, NJ, USA) and were
89 subsequently stored at -20 °C until further analysis. To determine the Chl *a* concentration, the samples were immersed in 8
90 mL of 90 % acetone overnight at 5 °C. Subsequently, 1 mL of the resulting solution was transferred to a 1.5 mL glass vial
91 (Mikrolab Aarhus A/S, Aarhus, Denmark) the following day and subjected to analysis using the Trilogy® Fluorometer
92 (Model #7200-00) equipped with a Chl *a* in vivo blue module (Model #7200-043, both Turner Designs, San Jose, CA, USA).
93 Measurements of serial dilutions from a 4 mg L⁻¹ stock standard and 90 % acetone (serving as blank) were performed to
94 calibrate the instrument. In addition, measurements of a solid-state secondary standard were performed every 10 samples.
95 Water (1 L) water from each depth was filtered for the determination of POC and PON concentrations, as well as natural
96 isotope abundance (δ ¹³C POC / δ ¹⁵N PON) using 47 mm ø, 0.7 μ m nominal pore size precombusted GF/F filter (GE
97 Healthcare Life Sciences, Whatman, USA), which were subsequently stored at -20 °C until further analysis. Seawater samples
98 for DNA were filtered through 47 mm ø, 0.22 μ m MCE membrane filter (Merck, Millipore Ltd., Ireland) for a maximum of 20
99 minutes, employing a gentle vacuum (200 mbar). The filtered volumes varied depending

100 on the amount of material captured on the filter, ranging from 1.3 L to 2 L, with precise measurements recorded. The filters
101 were promptly stored at -20 °C on the ship and moved to -80 °C upon arrival to the lab until further analysis.

102 To achieve detailed vertical profiles, a conductivity-temperature-depth-profiler (CTD, Seabird X) equipped with supplemen-
103 tary sensors for dissolved oxygen (DO), photosynthetic active radiation (PAR), and fluorescence (Fluorometer) was manually

104 deployed.

105 2.2 Nitrogen fixation and primary production

106
107 Water samples were collected at three distinct depths (0, 25 and 50 m) for the investigation of N₂ fixation rates and primary
108 production rates, encompassing the euphotic zone, chlorophyll maximum, and a light-absent zone. Three incubation stations
109 (Fig. 2: station 3, 7, 10) were chosen, in a way to cover the variability of the study area. This strategic sampling aimed to
110 capture a gradient of the water column with varying environmental conditions, relevant to the aim of the study. N₂ fixation
111 rates were assessed through triplicate incubations employing the modified ¹⁵N-N₂ dissolution technique after Großkopf et al.
112 (2012) and Mohr et al. (2010).

113 To ensure minimal contamination, 2.3 L glass bottles (Schott-Duran, Wertheim, Germany) underwent pre-cleaning and acid
114 washing before being filled with seawater samples. Oxygen contamination during sample collection was mitigated by gently
115 and bubble-free filling the bottles from the bottom, allowing the water to overflow. Each incubation bottle received a 100 mL
116 amendment of ¹⁵N-N₂ enriched seawater (98 %, Cambridge Isotope Laboratories, Inc., USA) achieving an average dissolved
117 N₂ isotope abundance (¹⁵N atom %) of 3.90 ± 0.02 atom % (mean \pm SD). Additionally, 1 mL of $H^{13}CO_3$ (1g/50 mL) (Sigma-
118 Aldrich, Saint Louis Missouri US) was added to each incubation bottle, roughly corresponding to 10 atom % enrichment and
119 thus measurements of primary production and N₂ fixation were conducted in the same bottle. Following the addition of both
120 isotopic components, the bottles were closed airtight with septa-fitted caps and incubated for 24 hours on-deck incubators with
121 a continuous surface seawater flow. These incubators, partially shaded (using daylight-filtering foil) to simulate in situ
122 photosynthetically active radiation (PAR) conditions, aimed to replicate environmental parameters experienced at the sampled
123 depths. Control incubations utilizing atmospheric air served as controls to monitor any natural changes in $\delta^{15}N$ not attributable
124 to ¹⁵N-N₂ addition. These control incubations were conducted using the dissolution method, like the ¹⁵N-N₂ enrichment
125 experiments, but with the substitution of atmospheric air instead of isotopic tracer.

126 After the incubation period, subsamples for nutrient analysis were taken from each incubation sample, and the remaining
127 content was subjected to the filtration process and were gently filtered (200 mbar) onto precombusted GF/F filters (Advantec,
128 47 mm ø, 0.7 μ m nominal pore size). This step ensured a comprehensive examination of both nutrient dynamics and the
129 isotopic composition of the particulate pool in the incubated samples. Samples were stored at -20 °C until further analysis.
130 Upon arrival in the lab, the filters were dried at 60 °C and to eliminate particulate inorganic carbon, subsequently subject to
131 acid fuming during which they were exposed to concentrated hydrochloric acid (HCL) vapors overnight in a desiccator. After
132 undergoing acid treatment, the filters were carefully dried, then placed into tin capsules and pelletized for subsequent analysis.
133 The determination of POC and PON, as well as isotopic composition ($\delta^{13}C$ POC / $\delta^{15}N$ PON), was carried out using an
134 elemental analyzer (Flash EA, ThermoFisher, USA) connected to a mass spectrometer (Delta V Advantage Isotope Ratio MS,
135 ThermoFisher, USA) with the ConFlo IV interface. This analytical setup was applied to all filters. These values, derived from
136 triplicate incubation measurements, exhibited no omission of data points or identification of outliers. Final rate calculations for
137 N₂ fixation rates were performed after Mohr et al. (2010) and primary production rates after Slawyk et al. (1977).

138 **2.3 Molecular methods**

139
140 The filters were flash-frozen in liquid nitrogen, crushed and DNA was extracted using the Qiagen DNA/RNA AllPrep Kit (Qi-
141 agen, Hildesheim, DE), following the procedure outlined by the manufacturer. The concentration and quality of the extracted
142 DNA was assessed spectrophotometrically using a MySpec spectrofluorometer (VWR, Darmstadt, Germany). The prepara-
143 tion of the metagenome library and sequencing were performed by BGI (China). Sequencing libraries were generated using
144 MGIEasy Fast FS DNA Library Prep Set following the manufacturer's protocol. Sequencing was conducted with 2x150bp on
145 a DNBSEQ-G400 platform (MGI). SOAPnuke1.5.5 (Chen et al. (2018)) was used to filter and trim low quality reads and
146 adaptor contaminants from the raw sequence reads, as clean reads. In total, fifteen metagenomic datasets were produced with
147 an average of 9.6G bp per sample.

148 **2.3.1 Metagenomic De Novo assembly, gene prediction, and annotation**

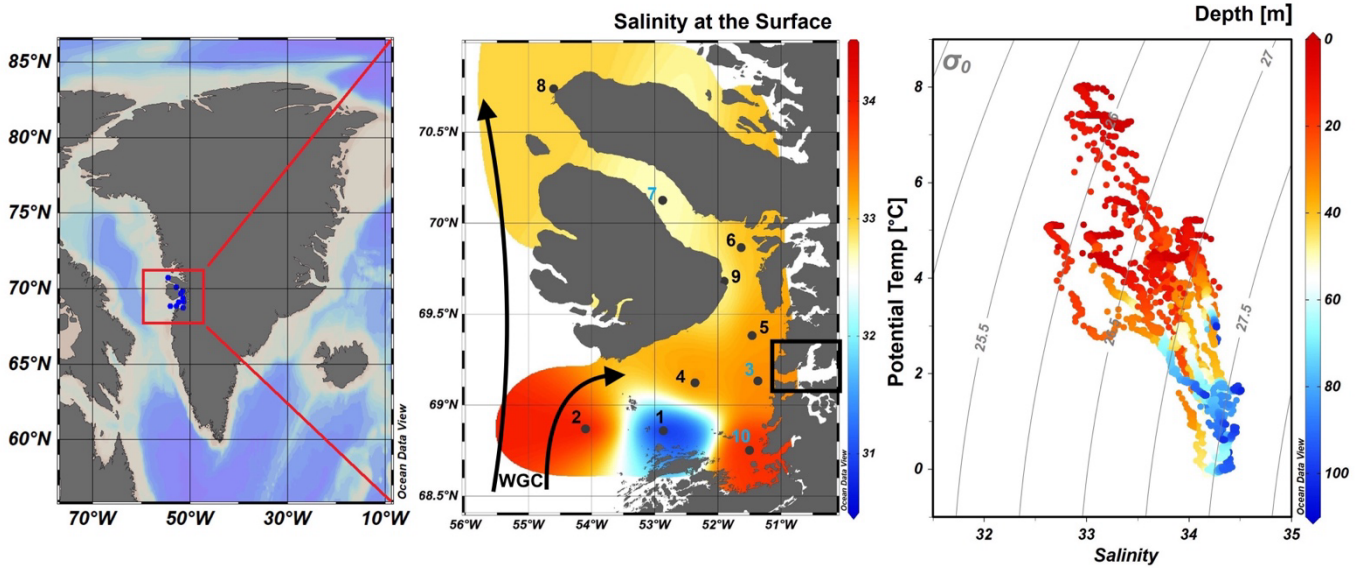
149
150 Megahit v1.2.9 (Li et al. (2015)) was used to assemble clean reads for each dataset with its minimum contig length as 500.
151 Prodigal v2.6.3 (Hyatt et al. (2010)) with the setting of “-p meta” was then used to predict the open reading frames (ORFs) of
152 the assembled contigs. ORFs from all the available datasets were filtered (>100bp), dereplicated and merged into a catalog of
153 non-redundant genes using cd-hit-est (>95 % sequence identity) (Fu et al. (2012)). Salmon v1.10.0 (Patro et al. (2017)) with
154 the “- meta” option was employed to map clean reads of each dataset to the catalog of non-redundant genes and generate the
155 GPM (genes per million reads) abundance. EggNOG mapper v2.1.12 (Cantalapiedra et al. (2021)) was then performed to assign
156 KEGG Orthology (KO) and identify specific functional annotation for the catalog of non-redundant genes. The marker genes,
157 *nifDK* (K02586, K02591 nitrogenase molybdenum-iron protein alpha/beta chain) and *nifH* (K02588, nitrogenase iron protein),
158 were used for the evaluation of microbial potential of N₂ fixation. *RbcL* (K01601, ribulose-bisphosphate carboxylase large
159 chain) and *psbA* (K02703, photosystem II P680 reaction center D1 protein) were selected to evaluate the microbial potential
160 of carbon fixation and photosynthesis, respectively. The molecular datasets have been deposited with the accession number:
161 Bioproject PRJNA1133027.

162 **3 Results and discussion**

163 **3.1 Hydrographic conditions in Qeqertarsuaq (Disco Bay) and Sullorsuaq (Vaigat) Strait**

164
165 Disko Bay (Qeqertarsuaq) is located along the west coast of Greenland (Kalaallit Nunaat) at approximately 69 °N (Figure 1),
166 and is strongly influenced by the West Greenland Current (WGC) which is associated with the broader Baffin Bay Polar Waters
167 (BBPW) (Mortensen et al., 2022; Hansen et al., 2012). The WGC does not only significantly shape the hydrographic conditions
168 within the bay but also plays an important role in the larger context of Greenland Ice Sheet melting (Mortensen et al. (2022)).
169 Central to the hydrographic system of the Qeqertarsuaq area is the Jakobshavn Isbræ, which is the most productive glacier in
170 the northern hemisphere and believed to drain about 7 % of the Greenland Ice Sheet and thus contributes substantially to the
171 water influx into the Qeqertarsuaq (Holland et al. (2008)). A predicted increased inflow of warm subsurface water, originating

173 from North Atlantic waters, has been suggested to further affect the melting of the Jakobshavn Isbræ and thus adds another
 174 layer of complexity to this dynamic system (Holland et al., 2008; Hansen et al., 2012).
 175 The hydrographic conditions in Qeqertarsuaq have a significant influence on biological processes, nutrient availability, and the

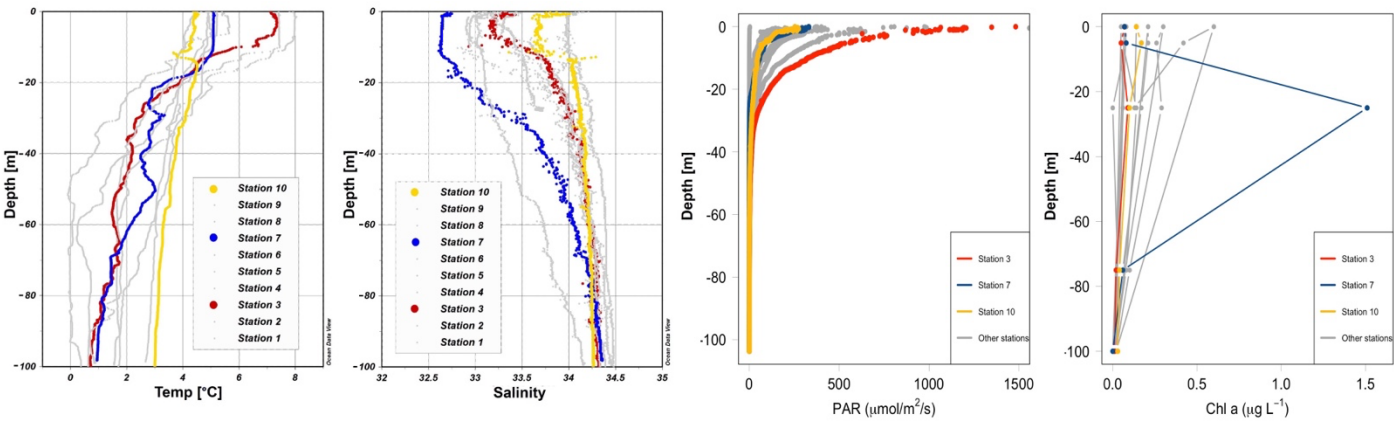


176
 177 **Figure 1.** Map of Greenland (Kalaallit Nunaat) with indication of study area (red box), on the left. Interpolated distribution of Sea Surface
 178 Salinity (SSS) values with corresponding isosurface lines and indication of 10 sampled stations (normal stations in black, incubation stations
 179 in blue), black arrows indicate the West Greenland Current (WGC) and the black box indicate the location of the Jakobshavn Isbræ, in the
 180 middle. Scatterplot of the potential temperature and salinity for all station data. The plot is used for the identification of the main water
 181 masses within the study area. Isopycnals (kg m^{-3}) are depicted in grey lines, on the right. Figures were created in Ocean Data View (ODV)
 182 (Schlitzer (2022)).

183 broader marine ecosystem (Munk et al., 2015; Hendry et al., 2019; Schiøtt, 2023).
 184

185 During our survey, we found very heterogenous hydrographic conditions at the different stations across Qeqertarsuaq (Fig. 1 &
 186 Fig. 2). The three selected stations for N_2 fixation analysis (stations 3, 7, and 10) were strategically chosen to capture the spatial
 187 variability of the area. Surface salinity and temperature measurements at these stations indicate the influence of freshwater
 188 input. The surface temperature exhibit a range of 4.5 to 8 °C, while surface salinity varies between 31 and 34, as illustrated in
 189 Fig. 1. The profiles sampled during our survey extend to a maximum depth of 100 m. Comparison of temperature/salinity (T/S)
 190 plots with recent studies suggests the presence of previously described water masses, including Warm Fjord Water (WFjW)
 191 and Cold Fjord Water (CFjW) with an overlaying surface glacial meltwater runoff. Those water masses are defined with a
 192 density range of $27.20 \leq \sigma_0 \leq 27.31$ but different temperature profiles. Thus water masses can be differentiated by their
 193 temperature within the same density range (Gladish et al. (2015)). Other water masses like upper subpolar mode water
 194 (uSPMW), deep subpolar mode water (dSPMW) and Baffin Bay polar Water (BBPW) which has been identified in the Disko

195 Bay (Qeqertarsuaq) before, cannot be identified from this data and may be present in deeper layers (Mortensen et al., 2022;
196 Sherwood et al., 2021; Myers and Ribergaard, 2013; Rysgaard et al., 2020). The temperature and salinity profiles across the 10



197
198
199
200 **Figure 2.** Profiles of temperature ($^{\circ}\text{C}$), salinity, photosynthetically active radiation (PAR) ($\mu\text{mol}/\text{m}^2/\text{s}$) and Chl a (mg m^{-3}) across stations 1 to
201 10 with depth (m). Stations 3, 7, and 10 are highlighted in red, blue, and yellow, respectively, to emphasize incubation stations. Figures were
202 created in Ocean Data View and R-Studio (Schlitzer (2022)).

203 stations in the study area show distinct stratification and variability, which is represented through the three incubation stations
204 (highlighted stations 3, 7, and 10 in Fig. 2). They display varying degrees of stratification and mixing, with notable differences
205 in the salinity and temperature profiles. Station 3 and station 7 exhibit clear stratification in both temperature and salinity
206 marked by the presence of thermoclines and haloclines. These features suggest significant freshwater input influenced by local
207 weather conditions and climate dynamics, like surface heat absorption. In contrast, Station 10 exhibits a narrower range of
208 temperature and salinity values throughout the water column compared to Stations 3 and 7, indicating more well-mixed
209 conditions. This uniformity is likely influenced by the regional circulation pattern and partial upwelling (Hansen et al., 2012;
210 Krawczyk et al., 2022). The distinct characteristics observed at station 10, as illustrated in the surface plot (Fig. 1), show an
211 elevated salinity and colder temperatures compared

212 to the other stations. This feature suggests upwelling of deeper waters along the shallower shelf, likely facilitated by the local
213 seafloor topography. Specifically, the seafloor shallowing off the coast of Station 10 may act as a barrier, disrupting typical
214 circulation and forcing deeper, saltier, and colder waters to the surface. This pattern aligns with previous studies that describe
215 similar mechanisms in the region (Krawczyk et al. (2022)). Their description of the bathymetry in Qeqertarsuaq, featuring
216 depths ranging from ca. 50 to 900 m, suggests its impact on turbulent circulation patterns, leading to the mixing of different
217 water masses. Evident variability in oceanographic conditions that can be observed throughout the study area occurs particularly
218 along characteristic topographical features like steep slopes, canyons, and shallower areas. The summer melting of sea ice and
219 glaciers introduces freshwater influxes that create distinct vertical and horizontal gradients in salinity and temperature in the
220 Qeqertarsuaq area Hansen et al. (2012). Additionally, the accelerated melting of the Jakobshavn Isbraæ, influenced by the

warmer inflow from the West Greenland Intermediate Current (WGIC), further alters the hydrographic conditions. Recent observations indicate significant warming and shoaling of the WGIC, potentially enabling it to overcome the sill separating the Illulissat Fjord from the Qeqertarsuaq area (Hansen et al., 2012; Holland et al., 2008; Myers and Ribergaard, 2013). This shift intensifies glacier melting, driving substantial changes in the local ecological dynamics (Ardyna et al., 2014; Arrigo et al., 2008; Bhatia et al., 2013).

3.2 Elevated N₂ fixation rates might play a role in nutrient dynamics and bloom development

We quantified N₂ fixation rates within the waters of Qeqertarsuaq, spanning from the surface to a depth of 50 m (Table 1). The rates ranged from 0.16 to 2.71 nmol N L⁻¹ d⁻¹ with all rates surpassing the detection limit. Our findings represent rates at the upper range of those observed in the Arctic Ocean. Previous measurements in the region have been limited, with only one study in Baffin Bay by Blais et al. (2012), reporting rates of 0.02 nmol N L⁻¹ d⁻¹, which are 1-2 orders of magnitude lower than our observations. Moreover, Sipler et al. (2017), reported rates in the coastal Chukchi Sea, with average values of 7.7 nmol N L⁻¹ d⁻¹. These values currently represent some of the highest rates measured in Arctic shelf environments. Compared to these, our highest measured rate (2.71 nmol N L⁻¹ d⁻¹) is slower, but still substantial, particularly considering the more Atlantic-influenced location of our study site. Sipler et al. (2017) also noted that a significant fraction of diazotrophs were <3 µm in size, suggesting that small unicellular diazotrophs play a dominant role in Arctic nitrogen fixation. Altogether, our data contribute to the growing evidence that N₂ fixation is a widespread and potentially significant nitrogen source across various Arctic regions. Simultaneous primary production rate measurements ranged from 0.07 to 3.79 µmol N L⁻¹ d⁻¹, with the highest rates observed at station 7 and generally higher values in the surface layers. Employing Redfield stoichiometry, the measured N₂ fixation rates accounted for 0.47 to 2.6 % (averaging 1.57 %) of primary production at our stations. The modest contribution to primary production suggests that N₂ fixation does not exert a substantial influence on the productivity of these waters during the time of the sampling. Rather, our N₂ fixation rates suggest primary production to depend mostly on additional nitrogen sources including regenerated, meltwater or land based sources.

The N:P ratio, calculated as DIN to DIP, indicates a deficit in N for primary production based on Redfield stoichiometry (Fig. 3). This aligns with findings presented by Jensen et al. (1999) and Tremblay and Gagnon (2009), who observed a similar nitrogen limitation in this region. Such biogeochemical conditions would be expected to generate a niche for N₂ fixing organisms (Sohm et al. (2011)). While N₂ fixation did not chiefly sustain primary production during our sampling campaign, we hypothesize that N₂ fixation has the potential to play a role in bloom dynamics. As nitrogen availability decreases

during a bloom, it may provide a niche for N₂ fixation, potentially extending the productive period of the bloom (Reeder et al. (2021)). Satellite data indicates that a fall bloom began in early August, following the annual spring bloom, as described by Ardyna et al. (2014). This double bloom situation may be driven by increased melting and the subsequent input of bioavailable nutrients and iron (Fe) from meltwater runoff (Arrigo et al., 2017; Hopwood et al., 2016; Bhatia et al., 2013). The meltwater from the Greenland Ice Sheet is a significant source of Fe (Bhatia et al., 2013; Hawkings et al., 2015, 2014), which is a limiting factor especially for diazotrophs (Sohm et al. (2011)). Consequently, it is possible that nutrients and Fe from the Isbræ glacier

introduced into the Qeqertarsuaq are promoting a bloom and further provide a niche for diazotrophs to thrive (Arrigo et al. (2017)).

Table 1. N_2 fixation ($\text{nmol N L}^{-1} \text{ d}^{-1}$), standard deviation (SD), primary productivity (PP; $\mu\text{mol C L}^{-1} \text{ d}^{-1}$), SD, percentage of estimated new primary productivity (% New PP) sustained by N_2 fixation, dissolved inorganic nitrogen compounds (NO_x), phosphorus (PO_4), and the molar nitrogen-to-phosphorus ratio (N:P) at stations 3, 7, and 10.

Station (no.)	Depth (m)	N_2 fixation ($\text{nmol N L}^{-1} \text{ d}^{-1}$)	SD (\pm)	Primary Productivity ($\mu\text{mol C L}^{-1} \text{ d}^{-1}$)	SD (\pm)	% New PP (%)	NO_x ($\mu\text{mol L}^{-1} \text{ d}^{-1}$)	PO_4 ($\mu\text{mol L}^{-1} \text{ d}^{-1}$)
3	0	1.20	0.21	0.466	0.08	1.71	0	0
3	25	1.88	0.11	0.588	0.04	2.11	0	0.70
3	50	0.29	0.01	0.209	0.00	0.91	0.33	1.48
7	0	2.49	0.44	0.63	0.20	2.60	0	0
7	25	2.71	0.22	3.79	2.45	0.47	0	0.45
7	50	0.53	0.24	0.33	0.36	1.08	0	0.97
10	0	1.48	0.12	0.74	0.15	1.33	0	0
10	25	0.31	0.01	0.29	0.07	0.73	0	0
10	50	0.16	0	0.07	0.07	1.40	0	0

A near-Redfield stoichiometry in POC:PON indicates that the particulate organic matter (POM) is freshly derived from an ongoing phytoplankton bloom, as phytoplankton generally assimilate carbon and nitrogen in relatively consistent proportions during active growth. In contrast, deviations from the Redfield ratio (e.g., elevated C:N or C:P) typically indicate microbial degradation and preferential remineralization of nitrogen and phosphorus (Redfield 1934; Geider and La Roche 2002; Sterner and Elser 2017). The absence of NO_x and the observed low N:P ratios suggest that nitrogen from earlier bloom phases has been largely depleted, potentially creating a niche for N_2 fixation as a supplementary nitrogen source. The onset and development of the bloom would be expected to lead to high nitrogen demands and intense competition for nitrogen sources. Notably, despite the apparent balance in the POM pool, the N:P ratio indicates strong nitrogen depletion and nutrient exhaustion within the ecosystem. This deficiency can be partly alleviated by N_2 fixation, providing possibly increasing amounts of nitrogen over the course of the bloom. Moreover, DIP is generally limited in the environment (Table 1); however, some organisms may still access it through luxury phosphorus uptake, storing excess phosphate when it is sporadically available. A recent study by Laso Perez et al. (2024) documented changes in microbial community composition during an Arctic bloom, focusing on nitrogen cycling. They observed a shift from chemolithotrophic to heterotrophic organisms throughout the summer bloom and noted increased activity to compete for various nitrogen sources. However, no *nifH* gene copies, indicative of nitrogen-fixing

organisms, were found in their dataset based on metagenome-assembled genomes (MAGs). This is not unexpected due to the classically low abundance of diazotrophs in marine microbial communities which has often been described (Turk-Kubo et al., 2015; Farnelid et al., 2019). Given the high productivity and metabolic activity observed in Qeqertarsuaq during a similar bloom period, the detected diazotrophs (Section 3.3) may play a more significant role than previously thought. Across the 10 stations there is considerable variability in POC and PON concentrations (Fig. 3). PON concentrations range from 0.0 $\mu\text{mol N L}^{-1}$ to 3.48 $\mu\text{mol N L}^{-1}$ (n=124), while POC concentrations range from 2.7 $\mu\text{mol C L}^{-1}$ to 27.2 $\mu\text{mol C L}^{-1}$ (n=144). The highest concentrations for both PON and POC were observed at station 7 at a depth of 25 m and coincide with the highest reported N_2 fixation rate (Figure Appendix A2 & A3). Generally, POC and PON concentrations decrease with depth, peaking at the deep chl *a* maximum (DCM), identified between 15 to 30 m across all stations. The DCM was identified based on measured chl *a* concentrations and previous descriptions in the region (Fox and Walker, 2022; Jensen et al., 1999). The variability in chl *a* concentrations indicates differences in phytoplankton abundance among the stations, with concentrations ranging between 0 to 0.42 mg m^{-3} . Excluding station 7, which exhibited the highest chl *a* concentration at the DCM (1.51 mg m^{-3}). While Tang et al. (2019) found that N_2 fixation measurements strongly correlated to satellite estimates of chl *a* concentrations, our results did not show a statistically significant correlation between nitrogen fixation rates and chl *a* concentrations overall (Figures A2 & A3). However, as noted, Station 7 at 25 m represents a unique case. The elevated concentration of chl *a* at this station likely resulted from a local phytoplankton bloom induced by meltwater outflow from the Isbræ glacier and sea ice melting, which may help explain the observed nitrogen fixation rates (Arrigo et al., 2017; Wang et al., 2014). This study's findings are in agreement with prior reports of analogous blooms occurring in the region (Fox and Walker, 2022; Jensen et al., 1999).

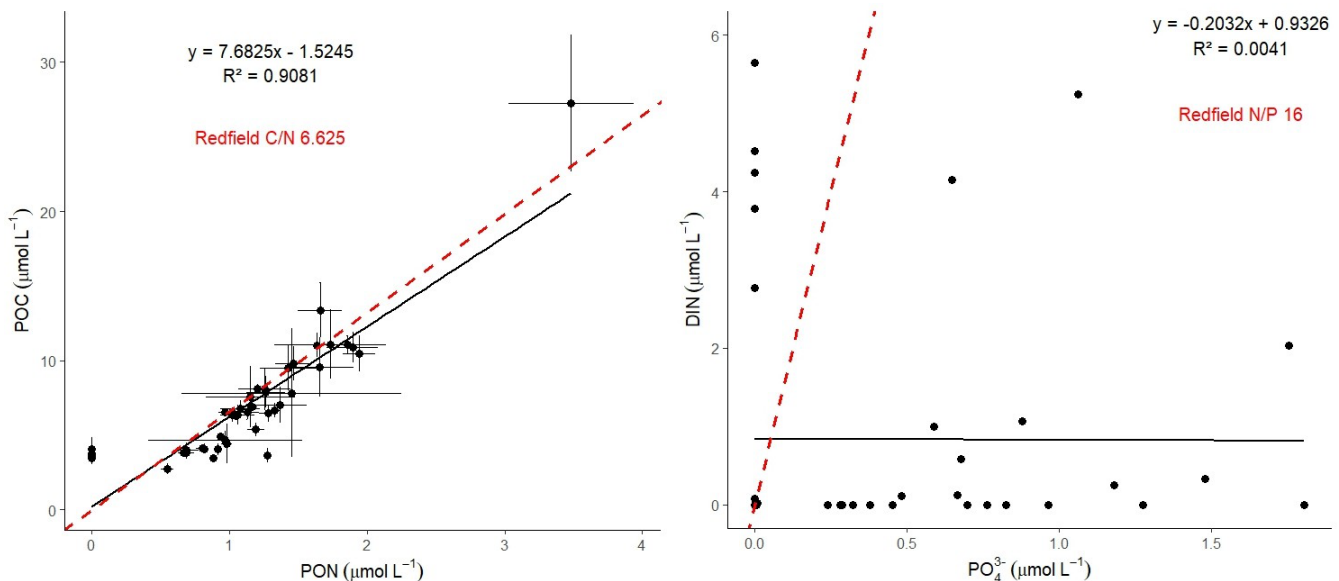


Figure 3. The POC/PON and DIN/DIP ratios at all 10 stations. The red line represents the Redfield ratios of POC/PON (106:16) and DIN/DIP (16:1).

301

302 **3.3 Potential Contribution of UCYN-A to Nitrogen Fixation During a Diatom Bloom: Insights and Uncertainties**

303 In our metagenomic analysis, we filtered the *nifH*, *nifD*, *nifK* genes, which code for the nitrogenase enzyme responsible for
 304 catalyzing N₂ fixation. We could identify sequences related to UCYN-A, which dominated the sequence pool of diazotrophs,
 305 particularly in the upper water masses (0 to 5 m) (Fig. 4). UCYN-A, a unicellular cyanobacterial symbiont, has a cosmopolitan
 306 distribution and is thought to substantially contribute to global N₂ fixation, as documented by (Martínez-Pérez et al., 2016;
 307 Tang et al., 2019). This conclusion is based on our metagenomic analysis, in which we set a sequence identity threshold of
 308 95% for both *nif* and photosystem genes. Notably, we only recovered sequences related to UCYN-A within our *nif* sequence
 309 pool, suggesting its predominance among detected diazotrophs. However, metagenomic approaches may underestimate overall
 310 diazotroph diversity, and we cannot fully exclude the presence of other, less abundant diazotrophs that may have been missed
 311 using this method. While UCYN-A was primarily detected in surface waters, we also observed relatively high *nifK* values at
 312 S3_100m, an unusual finding given that UCYN-A is typically constrained to the euphotic zone. Previous studies have
 313 predominantly reported UCYN-A in surface waters; for instance Harding et al. (2018) and Shiozaki et al. (2017) detected
 314 UCYN-A exclusively in the upper layers of the Arctic Ocean. Additionally, Shiozaki et al. (2020) found UCYN-A2 at depths
 315 extending to the 0.1% light level but not below 66 m in the Chukchi Sea. The detection of UCYN-A at 100 m in our study
 316 suggests that alternative mechanisms, such as particle association, vertical transport, or local environmental conditions, may
 317 facilitate its presence at depth. This warrants further investigation into the potential processes enabling its occurrence below
 318 the euphotic zone.

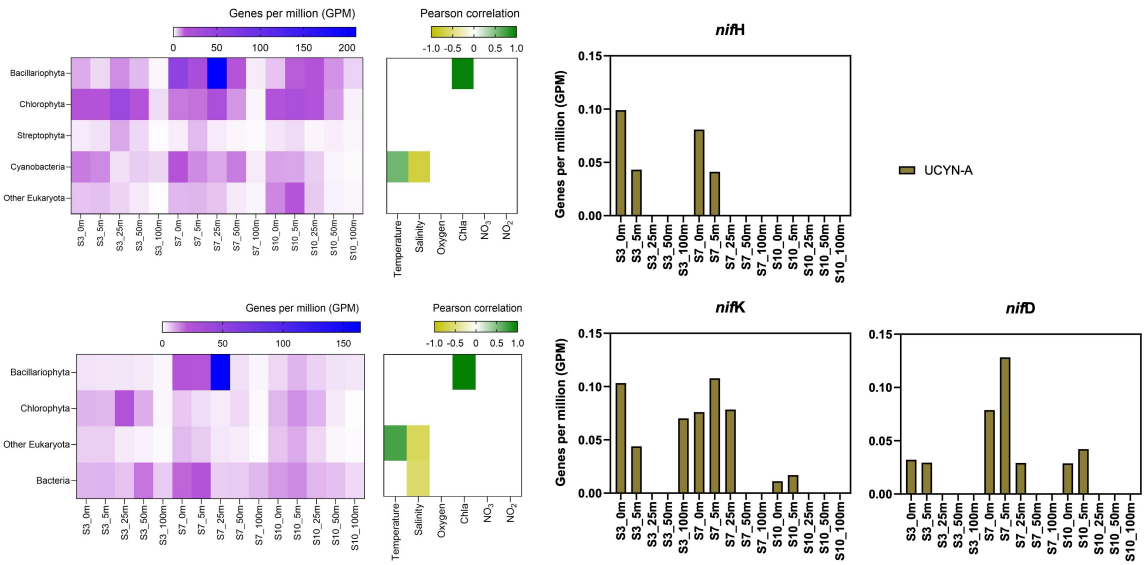
320 Due to the lack of genes such as those encoding Photosystem II and Rubisco, UCYN-A plays a significant role within the host
 321 cell and participates in fundamental cellular processes. Consequently it has evolved to become a closely integrated component
 322 of the host cell. Very recent findings demonstrate that UCYN-A imports proteins encoded by the host genome and has been
 323 described as an early form of N₂ fixing organelle termed a "Nitroplast" (Coale et al. (2024)).

324 Previous investigations document that they are critical for primary production, supplying up to 85% of the fixed nitrogen to their
 325 haptophyte host (Martínez-Pérez et al. (2016)). In addition to its high contribution to primary production, studies have shown
 326 that UCYN-A in high latitude waters fix similar amounts of N₂ per cell as in the tropical Atlantic Ocean, even in nitrogen-
 327 replete waters (Harding et al., 2018; Shiozaki et al., 2020; Martínez-Pérez et al., 2016; Krupke et al., 2015; Mills et al., 2020).
 328 However, estimating their contribution to N₂ fixation in our study is challenging, particularly since we detected cyanobacteria
 329 only at the surface but observe significant N₂ fixation rates below 5 m. The diazotrophic community is often underrepresented
 330 in metagenomic datasets due to the low abundance of nitrogenase gene copies, implying our data does not present a complete
 331 picture. We suspect a more diverse diazotrophic community exists, with UCYN-A being a significant contributor to N₂ fixation
 332 in Arctic waters. However, the exact proportion of its contribution requires further investigation.

333 The contribution of N₂ fixation to carbon fixation (as percent of PP) is relatively low, at the time of our study. We identified
 334 genes such as *rbcL*, which encodes Rubisco, a key enzyme in the carbon fixation pathway and *psbA*, a gene encoding
 335 Photosystem II, involved in light-driven electron transfer in photosynthesis, in our metagenomic dataset. The gene *rbcL* (for the

336 carbon fixation pathway) and the gene *psbA* (for primary producers) were used to track the community of photosynthetic primary
337 producers in our metagenomic dataset. At station 7, elevated carbon fixation rates are correlated with high diatom
338 (*Bacillariophyta*) abundance and increased chl *a* concentration (Fig. 4), suggesting the onset of a bloom, which is also
339 observable via satellite images (Appendix A1). We hypothesize that meltwater, carrying elevated nutrient and trace metal
340 concentrations, was rapidly transported away from the glacier through the Vaigat Strait by strong winds, leading to increased
341 productivity, as previously described by Fox and Walker (2022) & Jensen et al. (1999). The elevated diatom abundance and
342 primary production rates at station 7 coincide with the highest N₂ fixation rates, which could possibly point toward a possible
343 diatom-diazotroph symbiosis (Foster et al., 2022, 2011; Schvarcz et al., 2022). However, we did not detect a clear diazotrophic
344 signal directly associated with the diatoms in our metagenomic dataset, which might be due to generally underrepresentation of
345 diazotrophs in metagenomes due to low abundance or low sequencing coverage. To investigate this further, we examined
346 the taxonomic composition of *Bacillariophyta* at higher resolution. Among the various abundant diatom genera,
347 *Rhizosolenia* and *Chaetoceros* have been identified as symbiosis with diazotrophs (Grosse, et al., 2010; Foster, et al.,
348 2010), representing less than 6% or 15% of *Bacillariophyta*, based on *rbcL* or *psbA*, respectively (Figure Appendix A4).
349 Although we underestimate diazotrophs to an extent, the presence of certain diatom-diazotroph symbiosis could help
350 explain the high nitrogen fixation rates in the diatom bloom to a certain degree. Compilation of *nif* sequences identified
351 from this study as well as homologous from their NCBI top hit were added in Table S1. However, we cannot tell if the
352 diazotrophs belong to UCYN-A1 or UCYN-A2, or UCYN-A3. Based on the Pierella Karlusich et al. (2021), they
353 generated clonal *nifH* sequences from Tara Oceans, which the length of *nifH* sequences is much shorter than the two
354 *nifH* sequences we generated in our study. Also, the available UCYN-A2 or UCYN-A3 *nifH* sequences from NCBI were
355 shorter than the two *nifH* sequences we generated. Therefore, it would be not accurate to assign the *nifH* sequences to
356 either group under UCYN-A. Furthermore, not much information is available regarding the different groups of UCYN-
357 A using marker genes of *nifD* and *nifK*.

358



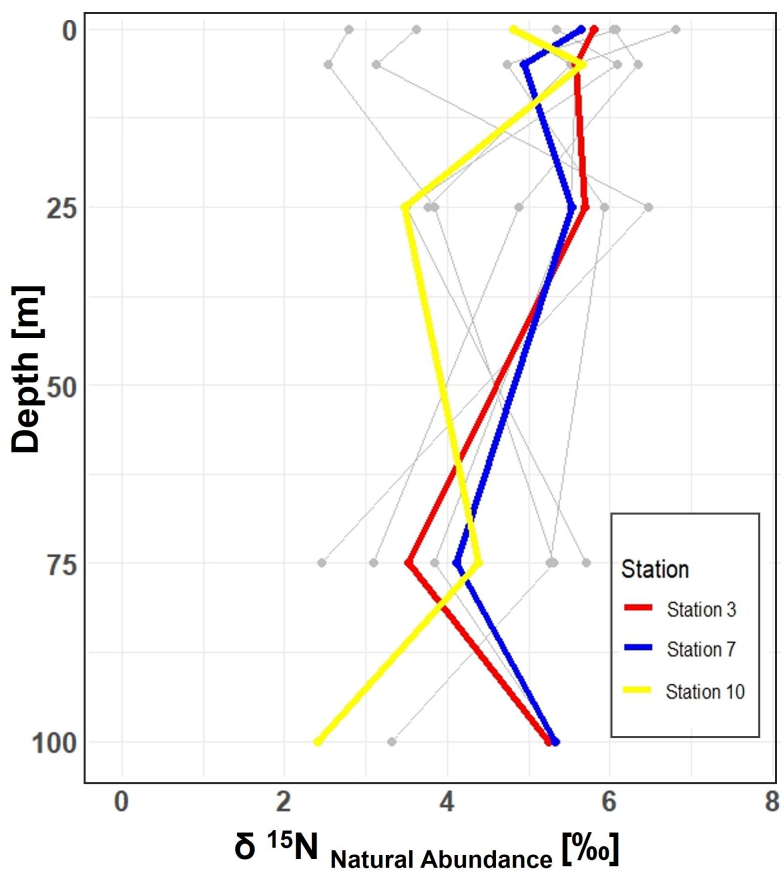
359
360
361
362 **Figure 4.** Upper left image: *psbA* with correlation plot. Lower left image: *rbcL* with correlation plot. Right image: *nifH*, *nifD*, *nifK* genes
363 per million reads in the metagenomic datasets. All figures display molecular data from metagenomic dataset for all sampled depth of station
364 3,7,10

365
366 There is evidence that UCYN-A have a higher Fe demand, with input through meltwater or river runoff potentially being
367 advantageous to those organisms (Shiozaki et al., 2017, 2018; Cheung et al., 2022). Consequently, UCYN-A might play a
368 more critical role in the future with increased Fe-rich meltwater runoff. UCYN-A can potentially fuel primary productivity by
369 supplying nitrogen, especially with increased melting, nutrient inputs, and more light availability due to rising temperatures as-
370 sociated with climate change. This predicted enhancement of primary productivity may contribute to the biological drawdown
371 of CO₂, acting as a negative feedback mechanism. These projections are based on studies forecasting increased temperatures,
372 melting, and resulting biogeochemical changes leading to higher primary productivity. However large uncertainties make pre-
373 dictions very difficult and should be handled with care. Thus we can only hypothesize that UCYN-A might be coupled to these
374 dynamics by providing essential nitrogen.

375 3.4 $\delta^{15}\text{N}$ Signatures in particulate organic nitrogen show no clear evidence of nitrogen fixation

376
377 Stable isotopic composition, expressed using the $\delta^{15}\text{N}$ notation, serve as indicators for understanding nitrogen dynamics
378 because different biogeochemical processes fractionate nitrogen isotopes in distinct ways (Montoya (2008)). However, it is
379 important to keep in mind that the final isotopic signal is a combination of all processes and an accurate distinction between
380 processes cannot be made. N₂ fixation tends to enrich nitrogenous compounds with lighter isotopes, producing OM with
381 isotopic values ranging approximately from -2 to +2 ‰ (Dähnke and Thamdrup (2013)). Upon complete remineralization and
382 oxidation, organic matter contributes to a reduction in the average δ -values in the open ocean (e.g. Montoya et al. (2002);

383 Emeis et al. (2010)). Whereas processes like denitrification and anammox preferentially remove lighter isotopes, leading to
384 enrichment in heavier isotopes and delta values up to -25 ‰.
385



386
387
388 **Figure 5.** Vertical profiles of $\delta^{15}\text{N}$ natural abundance signatures in PON across 10 stations in the study area. Incubation stations 3, 7, and 10
389 are highlighted in red, blue, and yellow, respectively. The figure shows variations in $\delta^{15}\text{N}$ signatures with depth at each station, providing
390 insight into nitrogen cycling in the study area.

391
392 Thus, $\delta^{15}\text{N}$ values help to identify different processes of the nitrogen cycle generally present in a system (Dähnke and Tham-
393 drup (2013)). In our study, the $\delta^{15}\text{N}$ values of PON from all 10 stations, range between 2.45 ‰ and 8.30 ‰ within the 0 to
394 100 m depth range, thus do not exhibit a clear signal indicative of N_2 fixation. This suggests that N_2 fixation likely contributes
395 only a certain fraction to export production or that it only started to contribute to isotope fractionation in the bloom dynamic.
396 The composition of OM in the surface ocean is influenced by the nitrogen substrate and the fractionation factor during
397 photosynthesis. When nitrate is depleted in the surface ocean, the isotopic signature of OM produced during photosynthesis will
398 mirror that of the nitrogen substrate. This substrate can originate from either nitrate in the subsurface or N_2 fixation. Notably,

399 nitrate, the primary form of dissolved nitrogen in the open ocean, typically exhibits an average stable isotope value of around
400 5 ‰. No fractionation occurs during photosynthesis because the nitrogen source is entirely taken up in the surface waters
401 (Sigman et al. (2009)). In Qeqertarsuaq, where similar conditions prevail, this suggests that factors other than N₂ fixation are
402 influencing the observed δ -values and POM is sustained by nitrogen sources from deeper subsurface waters, as observed in
403 earlier studies (Fox and Walker (2022)).

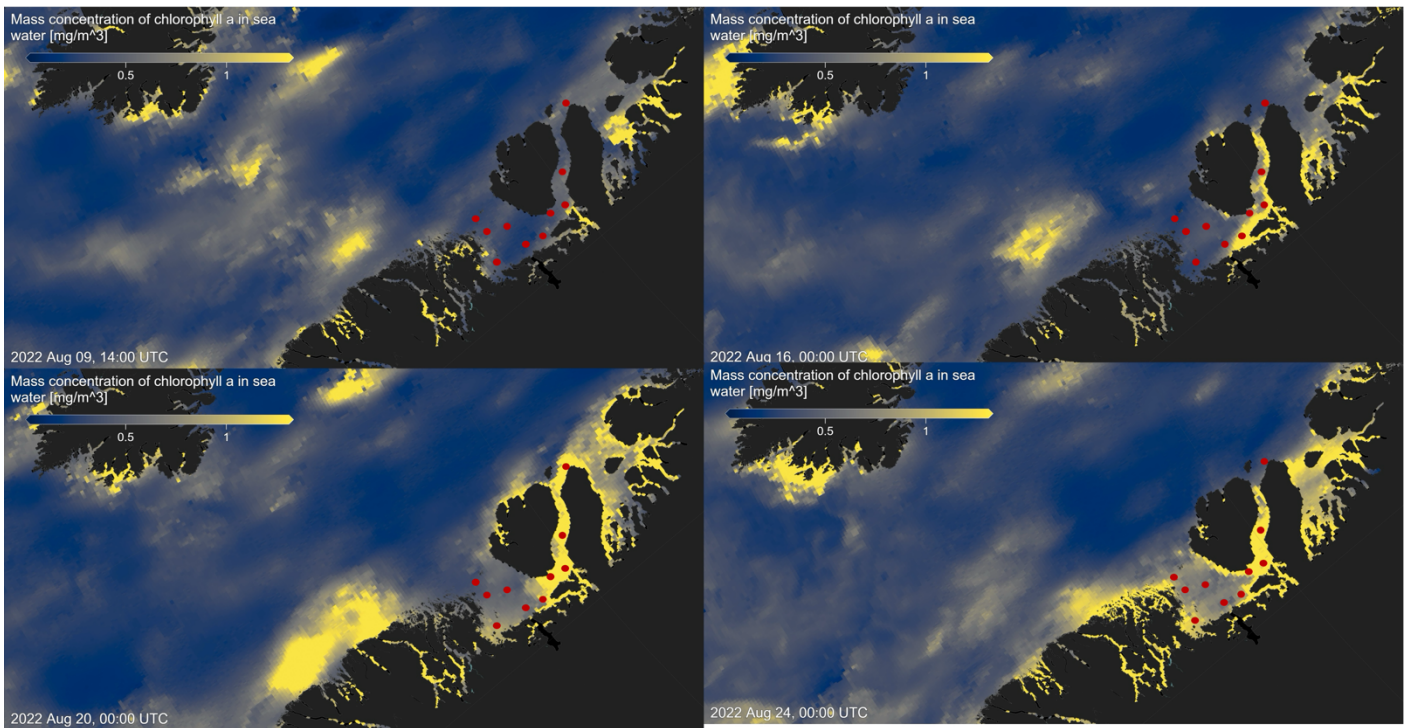
404 In the eastern Baffin Bay waters, Atlantic water masses serve as an important source of nitrate for sustaining primary productivity,
405 which is also reflected in the nitrogen isotopic signature in this study (Sherwood et al. (2021)). The influx of Atlantic
406 waters, characterized by NO₃⁻ values of approximately 5 ‰, closely matches the $\delta^{15}\text{N}$ values of observed PON concentrations
407 in our study. This suggests that Atlantic-derived NO₃⁻ serves as a primary source of new nitrogen to the initial stages of bloom
408 development (Fox and Walker, 2022; Knies, 2022). The mechanisms through which subsurface nitrate reaches the euphotic
409 layer are not well understood. However, potential pathways include vertical migration of phytoplankton and physical mixing.
410 Subsequently, nitrogen undergoes rapid recycling and remineralization processes to meet the system's nitrogen demands
411 (Jensen et al. (1999)).

412 413 4 Conclusion

414 Our study highlights the occurrence of elevated rates of N₂ fixation in Arctic coastal waters, particularly prominent at station 7,
415 where they coincide with high chl α values, indicative of heightened productivity. Satellite observations tracing the origin of a
416 bloom near the Isbræ Glacier, subsequently moving through the Vaigat strait, suggest a recurring phenomenon likely triggered
417 by increased nutrient-rich meltwater originating from the glacier. This aligns with previous reports by Jensen et al. (1999) &
418 Fox and Walker (2022), underlining the significance of such events in driving primary productivity in the region. The contribution
419 of N₂ fixation to primary production was low (average 1.57 %) across the stations. Since the demand was high relative to
420 the new nitrogen provided by N₂ fixation, the observed primary production must be sustained by the already present or adequate
421 amount of subsurface supply of NO_x nutrients in the seawater. This is also visible in the isotopic signature of the POM (Fox and
422 Walker, 2022; Sherwood et al., 2021). However, the detected N₂ fixation rates are likely linked to the development of the fresh
423 secondary summer bloom, which could be sustained by high nutrient and Fe availability from melting, potentially leading the
424 system into a nutrient-limited state. The ongoing high demand for nitrogen compounds may suggest an onset to further sustain
425 the bloom, but it remains speculative whether Fe availability definitively contributes to this process. The occurrence of such
426 double blooms has increased by 10 % in the Qeqertarsuaq and even 33 % in the Baffin Bay, with further projected increases
427 moving north from Greenland (Kalaallit Nunaat) waters (Ardyna et al. (2014)). Thus, nutrient demands are likely to increase,
428 and the role of N₂ fixation can become more significant. The diazotrophic community in this study is dominated by UCYN-A in
429 surface waters and may be linked to diatom abundance in deeper layers. This co-occurrence of diatoms and N₂ fixers in the
430 same location is probably due to the co-limitation of similar nutrients, rather than a symbiotic relationship. Thus, this highlights
431 the significant presence of diazotrophs despite their limited representation in datasets. It also highlights the potential for further
432

433 discoveries, as existing datasets likely underestimate the full extent of the diazotrophic community (Laso Perez et al., 2024;
434 Shao et al., 2023; Shiozaki et al., 2017, 2023). The reported N₂ fixation rates in the Vaigat strait within the Arctic Ocean are
435 notably higher than those observed in many other oceanic regions, emphasizing that N₂ fixation is an active and significant
436 process in these high-latitude waters. When compared to measured rates across various ocean systems using the ¹⁵N approach,
437 the significance of these findings becomes clear. For instance, N₂ fixation rates are sometimes below the detection limit and
438 often relatively low ranging from 0.8 to 4.4 nmol N L⁻¹ d⁻¹ (Löscher et al., 2020, 2016; Turk et al., 2011). In contrast, higher
439 rates reach up to 20 nmol N L⁻¹ d⁻¹ (Rees et al. (2009)) and sometime exceptional high rates range from 38 to 610 nmol N L⁻¹
440 d⁻¹ (Bonnet et al. (2009)). The Arctic Ocean rates are thus significant in the global context, underscoring the region's role in
441 the global nitrogen cycle and the importance of N₂ fixation in supporting primary productivity in these waters.
442 These findings highlight the urgent need to understand the interplay between seasonal variations, sea-ice dynamics, and hydro-
443 graphic conditions in Qeqertarsuaq. As climate change accelerates the melting of the Greenland Ice Sheet at Jakobshavn Isbrae,
444 shifts in hydrodynamic patterns and hydrographic conditions in Qeqertarsuaq are anticipated. The resulting influx of warmer
445 waters could significantly reshape the bay's hydrography, making it crucial to comprehend the coupling of climate-driven
446 changes and oceanic processes in this vital Arctic region. Our study provides key insights into these dynamics and underscores
447 the importance of continued investigation to predict Qeqertarsuaq's future hydrographic state. By detailing the environmental
448 and hydrographic changes, we contribute valuable knowledge to the broader context of N₂ fixation in the Arctic Ocean. Given
449 nitrogen's pivotal role in Arctic ecosystem productivity, it is essential to explore diazotrophs, quantify N₂ fixation, and assess
450 their impact on ecosystem services as climate change progresses.

451 **Appendix A**



454
455 **Figure A1.** Chlorophyll a concentration mg m^{-3} at four time points before, during, and after sea water sampling in August 2022
456 (sampling stations indicated by red dots), obtained from MODIS-Aqua; <https://giovanni.gsfc.nasa.gov> (Aqua MODIS Global Mapped Chl a
457 Data, version R2022.0, DOI:10.5067/AQUA/MODIS/L3M/CHL/2022), 4 km resolution, last access 03 June 2024

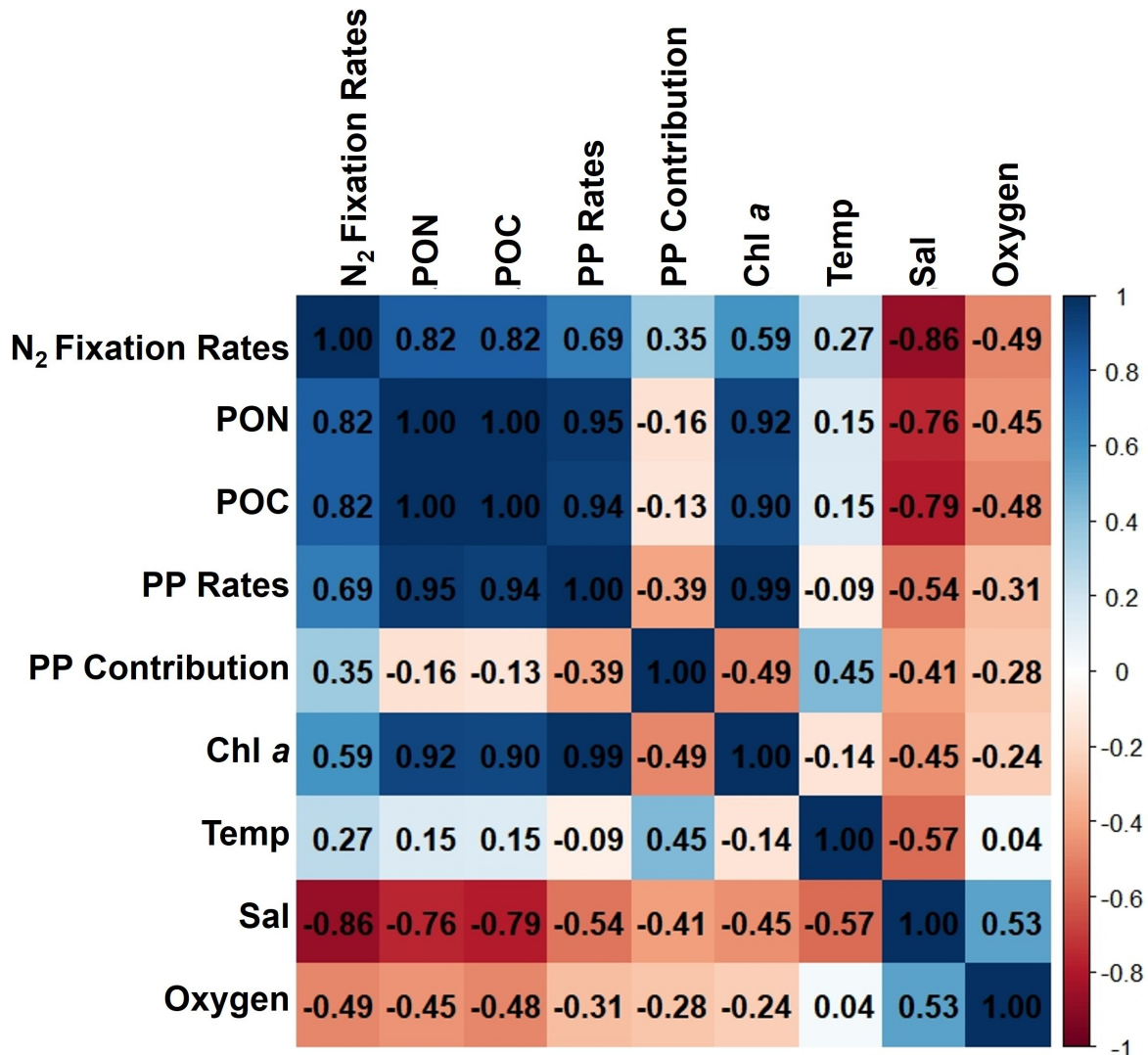


Figure A2. Correlation matrix of environmental and biological variables. The plot shows the correlation coefficients between the following parameters: N₂ fixation rates, PON, POC, PP rates, the contribution N₂ fixation to PP (PP contribution), Chl a, temperature (Temp), salinity (Sal), and Oxygen. The scale ranges from -1 to 1, where values close to 1 or -1 indicate strong positive or negative correlations, respectively, and values near 0 indicate weak or no correlation. The color intensity represents the strength and direction of the correlations, facilitating the identification of relationships among the variables

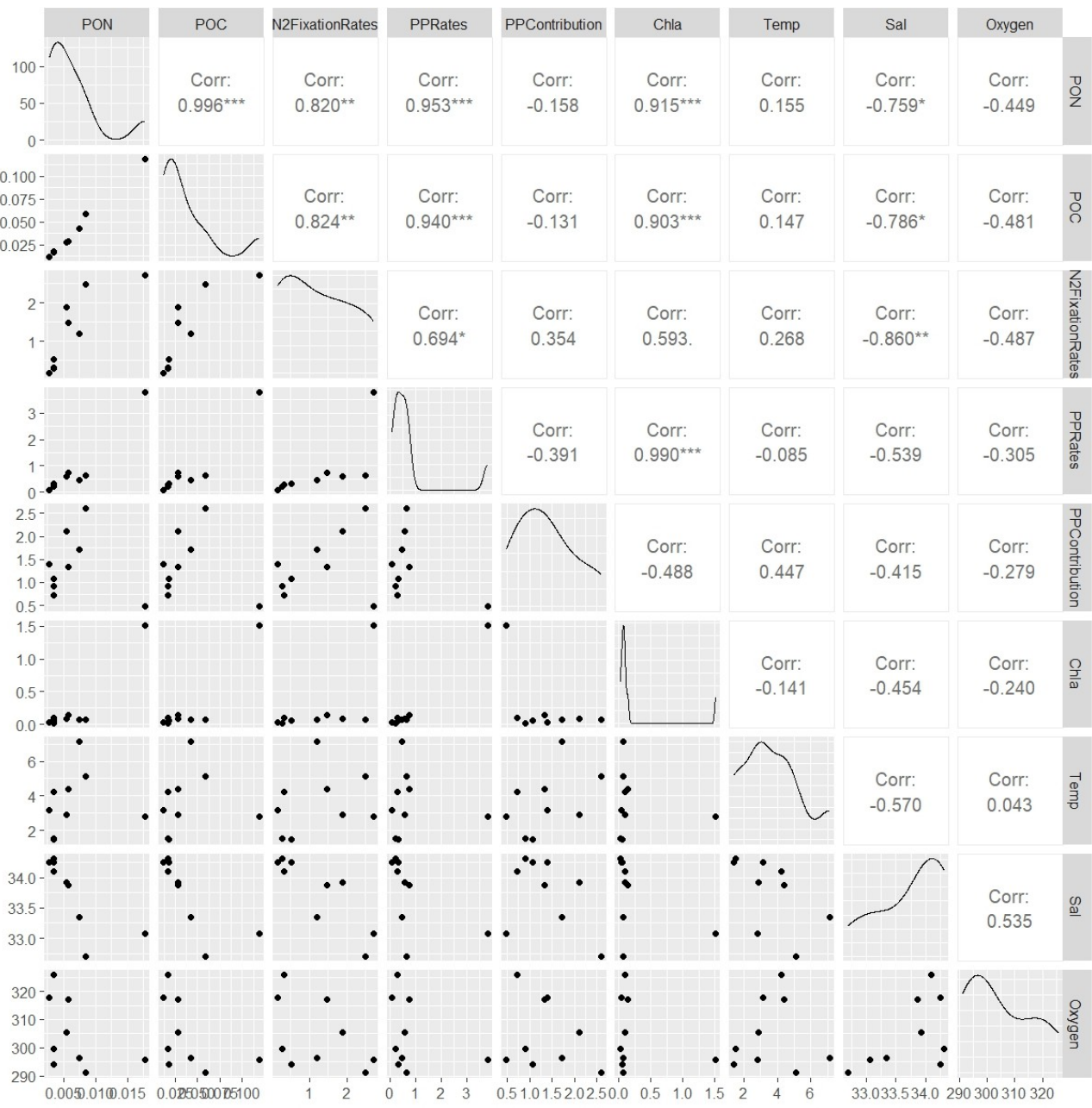


Figure A3. This figure displays a ggpairs plot, showing pairwise relationships and correlations between biological and environmental variables. Pearson correlation coefficients displayed in the upper triangular panel, indicating the strength and significance of linear relationships. Statistical significance levels are indicated by stars (*), where * indicates $p < 0.05$, ** indicates $p < 0.01$ and *** indicates $p < 0.001$.

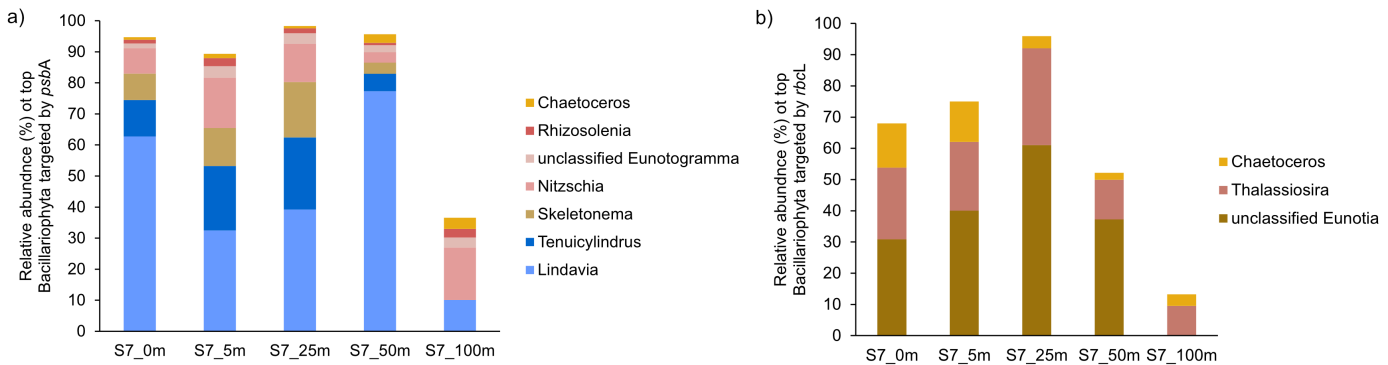


Figure A4. Taxonomic composition of Bacillariophyta at Station 7 based on a) psbA and b) rbcL marker genes. The figure shows the relative abundance of Bacillariophyta genera detected in the metagenomic dataset, grouped by gene-specific classifications.

479 *Data availability.* The presented data collected during the cruise will be made accessible on PANGEA. The molecular datasets have been
480 deposited with the accession number: Bioproject PRJNA1133027

Author contributions. IS carried out fieldwork and laboratory work at the University of Southern Denmark, and wrote the majority of the manuscript. ELP, AM, and EL conducted fieldwork and laboratory work at the University of Southern Denmark. PX performed metagenomic analysis and created the corresponding graphs. CRL designed the study, provided supervision and guidance throughout the project, and contributed to the writing and revision of the manuscript. All authors contributed to the conception of the study and participated in the writing and revision of the manuscript.

492 *Competing interests.* The authors declare that they have no known competing financial interests or personal relationships that could have
493 appeared to influence the work reported in this paper. One of the authors, CRL, serves as an Associate Editor for Biogeosciences.

497 *Acknowledgements.* This work was supported by the Velux Foundation (grant no.29411 to Carolin R. Löscher) and through the DFF grant
498 from the the Independent Research Fund Denmark (grant no. 0217-00089B to Lasse Riemann, Carolin R. Löscher and Stig Markager). ELP
499 was supported by a postdoctoral contract from Danmarks Frie Forskningsfond (DFF, 1026-00428B) at SDU, and by a Marie Skłodowska-
500 Curie postdoctoral fellowship (HORIZON2021 MSCA-2021-PF-01, project number: 101066750) by the European Commission at Princeton
501 University. We sincerely thank the captain and crew of the P540 during the cruise on the Danish military vessel for their invaluable support and
502 cooperation at sea. Our gratitude extends to Isaaffik Arctic Gateway for providing the infrastructure and opportunities that made this project
503 possible. We also acknowledge Zarah Kofoed for her technical support in the laboratory and thank all the Nordceo laboratory technicians for

504 their general assistance.

505 References

506 Ardyna, M. and Arrigo, K. R.: Phytoplankton dynamics in a changing Arctic Ocean, *Nature Climate Change*, 10, 892–903, 2020.

507 Ardyna, M., Babin, M., Gosselin, M., Devred, E., Rainville, L., and Tremblay, J.-É.: Recent Arctic Ocean sea ice loss triggers novel fall
508 phytoplankton blooms, *Geophysical Research Letters*, 41, 6207–6212, 2014.

509 Arrigo, K. R. and van Dijken, G. L.: Continued increases in Arctic Ocean primary production, *Progress in oceanography*, 136, 60–70, 2015.

510 Arrigo, K. R., van Dijken, G., and Pabi, S.: Impact of a shrinking Arctic ice cover on marine primary production, *Geophysical Research
511 Letters*, 35, 2008.

512 Arrigo, K. R., van Dijken, G. L., Castelao, R. M., Luo, H., Rennermalm, Å. K., Tedesco, M., Mote, T. L., Oliver, H., and Yager, P. L.:
513 Melting glaciers stimulate large summer phytoplankton blooms in southwest Greenland waters, *Geophysical Research Letters*, 44, 6278–
514 6285, 2017.

515 Bhatia, M. P., Kujawinski, E. B., Das, S. B., Breier, C. F., Henderson, P. B., and Charette, M. A.: Greenland meltwater as a significant and
516 potentially bioavailable source of iron to the ocean, *Nature Geoscience*, 6, 274–278, 2013.

517 Blais, M., Tremblay, J.-É., Jungblut, A. D., Gagnon, J., Martin, J., Thaler, M., and Lovejoy, C.: Nitrogen fixation and identification of
518 potential diazotrophs in the Canadian Arctic, *Global Biogeochemical Cycles*, 26, 2012.

519 Bonnet, S., Biegala, I. C., Dutrieux, P., Slemons, L. O., and Capone, D. G.: Nitrogen fixation in the western equatorial Pacific: Rates,
520 diazotrophic cyanobacterial size class distribution, and biogeochemical significance, *Global Biogeochemical Cycles*, 23, 2009.

521 Buchanan, P. J., Chase, Z., Matear, R. J., Phipps, S. J., and Bindoff, N. L.: Marine nitrogen fixers mediate a low latitude pathway for
522 atmospheric CO₂ drawdown, *Nature Communications*, 10, 4611, 2019.

523 Cantalapiedra, C. P., Hernández-Plaza, A., Letunic, I., Bork, P., and Huerta-Cepas, J.: eggNOG-mapper v2: functional annotation, orthology
524 assignments, and domain prediction at the metagenomic scale, *Molecular biology and evolution*, 38, 5825–5829, 2021.

525 Capone, D. G. and Carpenter, E. J.: Nitrogen fixation in the marine environment, *Science*, 217, 1140–1142, 1982.

526 Chen, Y., Chen, Y., Shi, C., Huang, Z., Zhang, Y., Li, S., Li, Y., Ye, J., Yu, C., Li, Z., et al.: SOAPnuke: a MapReduce acceleration-supported
527 software for integrated quality control and preprocessing of high-throughput sequencing data, *Gigascience*, 7, gix120, 2018.

528 Cheung, S., Liu, K., Turk-Kubo, K. A., Nishioka, J., Suzuki, K., Landry, M. R., Zehr, J. P., Leung, S., Deng, L., and Liu, H.: High biomass
529 turnover rates of endosymbiotic nitrogen-fixing cyanobacteria in the western Bering Sea, *Limnology and Oceanography Letters*, 7, 501–
530 509, 2022.

531 Coale, T. H., Loconte, V., Turk-Kubo, K. A., Vanslembrouck, B., Mak, W. K. E., Cheung, S., Ekman, A., Chen, J.-H., Hagino, K., Takano,
532 Y., et al.: Nitrogen-fixing organelle in a marine alga, *Science*, 384, 217–222, 2024.

533 Dähnke, K. and Thamdrup, B.: Nitrogen isotope dynamics and fractionation during sedimentary denitrification in Boknis Eck, Baltic Sea,
534 Biogeosciences, 10, 3079–3088, 2013.

535 Damm, E., Helmke, E., Thoms, S., Schauer, U., Nöthig, E., Bakker, K., and Kiene, R.: Methane production in aerobic oligotrophic surface
536 water in the central Arctic Ocean, *Biogeosciences*, 7, 1099–1108, 2010.

537 Díez, B., Bergman, B., Pedrós-Alió, C., Antó, M., and Snoeijs, P.: High cyanobacterial *nifH* gene diversity in Arctic seawater and sea ice
538 brine, *Environmental microbiology reports*, 4, 360–366, 2012.

539 Emeis, K.-C., Mara, P., Schlarbaum, T., Möbius, J., Dähnke, K., Struck, U., Mihalopoulos, N., and Krom, M.: External N inputs and internal
540 N cycling traced by isotope ratios of nitrate, dissolved reduced nitrogen, and particulate nitrogen in the eastern Mediterranean Sea, *Journal
541*

542 of Geophysical Research: Biogeosciences, 115, 2010.

543 Falkowski, P. G., Fenchel, T., and Delong, E. F.: The microbial engines that drive Earth's biogeochemical cycles, science, 320, 1034–1039,
544 2008.

545 Farnelid, H., Andersson, A. F., Bertilsson, S., Al-Soud, W. A., Hansen, L. H., Sørensen, S., Steward, G. F., Hagström, Å., and Riemann, L.:
546 Nitrogenase gene amplicons from global marine surface waters are dominated by genes of non-cyanobacteria, *PloS one*, 6, e19 223, 2011.

547 Farnelid, H., Turk-Kubo, K., Ploug, H., Ossolinski, J. E., Collins, J. R., Van Mooy, B. A., and Zehr, J. P.: Diverse diazotrophs are present on
548 sinking particles in the North Pacific Subtropical Gyre, *The ISME journal*, 13, 170–182, 2019.

549 Fernández-Méndez, M., Turk-Kubo, K. A., Buttigieg, P. L., Rapp, J. Z., Krumpen, T., and Zehr, J. P.: Diazotroph diversity in the sea ice, melt
550 ponds, and surface waters of the Eurasian Basin of the Central Arctic Ocean, *Frontiers in microbiology*, 7, 217 140, 2016.

551 Foster, R. A., Goebel, N. L., & Zehr, J. P.: Isolation of calothrix rhizosoleniae (cyanobacteria) strain SC01 from *chaetoceros*
552 (bacillariophyta) spp. diatoms of the subtropical north pacific ocean 1. *Journal of Phycology*, 46(5), 1028-1037, 2010.

553 Foster, R. A., Kuypers, M. M., Vagner, T., Paerl, R. W., Musat, N., and Zehr, J. P.: Nitrogen fixation and transfer in open ocean diatom–
554 cyanobacterial symbioses, *The ISME journal*, 5, 1484–1493, 2011.

555 Foster, R. A., Tienken, D., Littmann, S., Whitehouse, M. J., Kuypers, M. M., and White, A. E.: The rate and fate of N2 and C fixation by
556 marine diatom-diazotroph symbioses, *The ISME journal*, 16, 477–487, 2022.

557 Fox, A. and Walker, B. D.: Sources and Cycling of Particulate Organic Matter in Baffin Bay: A Multi-Isotope $\delta^{13}\text{C}$, $\delta^{15}\text{N}$, and $\Delta^{14}\text{C}$
558 Approach, *Frontiers in Marine Science*, 9, 846 025, 2022.

559 Fu, L., Niu, B., Zhu, Z., Wu, S., and Cd-hit, W. L.: Accelerated for clustering the next-generation sequencing data, *Bioinformatics*, 28,
560 3150–3152, 2012.

561 Galloway, J., Dentener, F., Capone, D., Boyer, E., Howarth, R., Seitzinger, S., Asner, G., Cleveland, C., Green, P., Holland, E., et al.: Nitrogen
562 cycles: past, present, and future. *Biogeochemistry* 70, 153e226, 2004.

563 García-Robledo, E., Corzo, A., and Papaspyrou, S.: A fast and direct spectrophotometric method for the sequential determination of nitrate
564 and nitrite at low concentrations in small volumes, *Marine Chemistry*, 162, 30–36, 2014.

565 Geider, R. J., & La Roche, J.: Redfield revisited: variability of C [ratio] N [ratio] P in marine microalgae and its biochemical
566 basis. *European Journal of Phycology*, 37(1), 1-17, 2002.

567 Gladish, C. V., Holland, D. M., and Lee, C. M.: Oceanic boundary conditions for Jakobshavn Glacier. Part II: Provenance and sources of
568 variability of Disko Bay and Ilulissat icefjord waters, 1990–2011, *Journal of Physical Oceanography*, 45, 33–63, 2015.

569 Grosse, J., Bombar, D., Doan, H. N., Nguyen, L. N., & Voss, M.: The Mekong River plume fuels nitrogen fixation and determines
570 phytoplankton species distribution in the South China Sea during low and high discharge season. *Limnology and Oceanography*, 55(4),
571 1668-1680, 2010.

572 Großkopf, T., Mohr, W., Baustian, T., Schunck, H., Gill, D., Kuypers, M. M., Lavik, G., Schmitz, R. A., Wallace, D. W., and LaRoche, J.:
573 Doubling of marine dinitrogen-fixation rates based on direct measurements, *Nature*, 488, 361–364, 2012.

574 Gruber, N.: The dynamics of the marine nitrogen cycle and its influence on atmospheric CO₂ variations, in: *The ocean carbon cycle and*
575 *climate*, pp. 97–148, Springer, 2004.

576 Gruber, N. and Galloway, J. N.: An Earth-system perspective of the global nitrogen cycle, *Nature*, 451, 293–296, 2008.

577 Gruber, N. and Sarmiento, J. L.: Global patterns of marine nitrogen fixation and denitrification, *Global biogeochemical cycles*, 11, 235–266,
578 1997.

579 Haine, T. W., Curry, B., Gerdes, R., Hansen, E., Karcher, M., Lee, C., Rudels, B., Spreen, G., de Steur, L., Stewart, K. D., et al.: Arctic
580 freshwater export: Status, mechanisms, and prospects, *Global and Planetary Change*, 125, 13–35, 2015.

581 Hanna, E., Huybrechts, P., Steffen, K., Cappelen, J., Huff, R., Shuman, C., Irvine-Fynn, T., Wise, S., and Griffiths, M.: Increased runoff from
582 melt from the Greenland Ice Sheet: a response to global warming, *Journal of Climate*, 21, 331–341, 2008.

583 Hansen, M. O., Nielsen, T. G., Stedmon, C. A., and Munk, P.: Oceanographic regime shift during 1997 in Disko Bay, western Greenland,
584 *Limnology and Oceanography*, 57, 634–644, 2012.

585 Harding, K., Turk-Kubo, K. A., Sipler, R. E., Mills, M. M., Bronk, D. A., and Zehr, J. P.: Symbiotic unicellular cyanobacteria fix nitrogen in
586 the Arctic Ocean, *Proceedings of the National Academy of Sciences*, 115, 13 371–13 375, 2018.

587 Hawkings, J., Wadham, J., Tranter, M., Lawson, E., Sole, A., Cowton, T., Tedstone, A., Bartholomew, I., Nienow, P., Chandler, D., et al.:
588 The effect of warming climate on nutrient and solute export from the Greenland Ice Sheet, *Geochemical Perspectives Letters*, pp. 94–104,
589 2015.

590 Hawkings, J. R., Wadham, J. L., Tranter, M., Raiswell, R., Benning, L. G., Statham, P. J., Tedstone, A., Nienow, P., Lee, K., and Telling, J.:
591 Ice sheets as a significant source of highly reactive nanoparticulate iron to the oceans, *Nature communications*, 5, 1–8, 2014.

592 Hendry, K. R., Huvenne, V. A., Robinson, L. F., Annett, A., Badger, M., Jacobel, A. W., Ng, H. C., Opher, J., Pickering, R. A., Taylor, M. L.,
593 et al.: The biogeochemical impact of glacial meltwater from Southwest Greenland, *Progress in Oceanography*, 176, 102 126, 2019.

594 Holland, D. M., Thomas, R. H., De Young, B., Ribergaard, M. H., and Lyberth, B.: Acceleration of Jakobshavn Isbræ triggered by warm
595 subsurface ocean waters, *Nature geoscience*, 1, 659–664, 2008.

596 Hopwood, M. J., Connelly, D. P., Arendt, K. E., Juul-Pedersen, T., Stinchcombe, M. C., Meire, L., Esposito, M., and Krishna, R.: Seasonal
597 changes in Fe along a glaciated Greenlandic fjord, *Frontiers in Earth Science*, 4, 15, 2016.

598 Hyatt, D., Chen, G.-L., LoCascio, P. F., Land, M. L., Larimer, F. W., and Hauser, L. J.: Prodigal: prokaryotic gene recognition and translation
599 initiation site identification, *BMC bioinformatics*, 11, 1–11, 2010.

600 Jensen, H. M., Pedersen, L., Burmeister, A., and Winding Hansen, B.: Pelagic primary production during summer along 65 to 72 N off West
601 Greenland, *Polar Biology*, 21, 269–278, 1999.

602 Karl, D., Michaels, A., Bergman, B., Capone, D., Carpenter, E., Letelier, R., Lipschultz, F., Paerl, H., Sigman, D., and Stal, L.: Dinitrogen
603 fixation in the world's oceans, *The nitrogen cycle at regional to global scales*, pp. 47–98, 2002.

604 Knies, J.: Nitrogen isotope evidence for changing Arctic Ocean ventilation regimes during the Cenozoic, *Geophysical Research Letters*, 49,
605 e2022GL099 512, 2022.

606 Krawczyk, D. W., Yesson, C., Knutz, P., Arboe, N. H., Blicher, M. E., Zinglersen, K. B., and Wagnholt, J. N.: Seafloor habitats across
607 geological boundaries in Disko Bay, central West Greenland, *Estuarine, Coastal and Shelf Science*, 278, 108 087, 2022.

608 Krupke, A., Mohr, W., LaRoche, J., Fuchs, B. M., Amann, R. I., and Kuypers, M. M.: The effect of nutrients on carbon and nitrogen fixation
609 by the UCYN-A–haptophyte symbiosis, *The ISME journal*, 9, 1635–1647, 2015.

610 Laso Perez, R., Rivas Santisteban, J., Fernandez-Gonzalez, N., Mundy, C. J., Tamames, J., and Pedros-Alio, C.: Nitrogen cycling during an
611 Arctic bloom: from chemolithotrophy to nitrogen assimilation, *bioRxiv*, pp. 2024–02, 2024.

612 Lewis, K., Van Dijken, G., and Arrigo, K. R.: Changes in phytoplankton concentration now drive increased Arctic Ocean primary production,
613 *Science*, 369, 198–202, 2020.

614 Li, D., Liu, C.-M., Luo, R., Sadakane, K., and Lam, T.-W.: MEGAHIT: an ultra-fast single-node solution for large and complex metagenomics
615 assembly via succinct de Bruijn graph, *Bioinformatics*, 31, 1674–1676, 2015.

616 Löscher, C. R., Bourbonnais, A., Dekaezemacker, J., Charoenpong, C. N., Altabet, M. A., Bange, H. W., Czeschel, R., Hoffmann, C., and
617 Schmitz, R.: N 2 fixation in eddies of the eastern tropical South Pacific Ocean, *Biogeosciences*, 13, 2889–2899, 2016.

618 Löscher, C. R., Mohr, W., Bange, H. W., and Canfield, D. E.: No nitrogen fixation in the Bay of Bengal?, *Biogeosciences*, 17, 851–864, 2020.

619 Luo, Y.-W., Doney, S., Anderson, L., Benavides, M., Berman-Frank, I., Bode, A., Bonnet, S., Boström, K. H., Böttjer, D., Capone, D., et al.:
620 Database of diazotrophs in global ocean: abundance, biomass and nitrogen fixation rates, *Earth System Science Data*, 4, 47–73, 2012.

621 Martínez-Pérez, C., Mohr, W., Löscher, C. R., Dekaezemacker, J., Littmann, S., Yilmaz, P., Lehnen, N., Fuchs, B. M., Lavik, G., Schmitz,
622 R. A., et al.: The small unicellular diazotrophic symbiont, UCYN-A, is a key player in the marine nitrogen cycle, *Nature Microbiology*, 1,
623 1–7, 2016.

624 Mills, M. M., Turk-Kubo, K. A., van Dijken, G. L., Henke, B. A., Harding, K., Wilson, S. T., Arrigo, K. R., and Zehr, J. P.: Unusual marine
625 cyanobacteria/haptophyte symbiosis relies on N2 fixation even in N-rich environments, *The ISME Journal*, 14, 2395–2406, 2020.

626 Mohr, W., Grosskopf, T., Wallace, D. W., and LaRoche, J.: Methodological underestimation of oceanic nitrogen fixation rates, *PloS one*, 5,
627 e12 583, 2010.

628 Montoya, J. P.: Nitrogen stable isotopes in marine environments, *Nitrogen in the marine environment*, 2, 1277–1302, 2008.

629 Montoya, J. P., Carpenter, E. J., and Capone, D. G.: Nitrogen fixation and nitrogen isotope abundances in zooplankton of the oligotrophic
630 North Atlantic, *Limnology and Oceanography*, 47, 1617–1628, 2002.

631 Mortensen, J., Rysgaard, S., Winding, M., Juul-Pedersen, T., Arendt, K., Lund, H., Stuart-Lee, A., and Meire, L.: Multidecadal water mass
632 dynamics on the West Greenland Shelf, *Journal of Geophysical Research: Oceans*, 127, e2022JC018 724, 2022.

633 Munk, P., Nielsen, T. G., and Hansen, B. W.: Horizontal and vertical dynamics of zooplankton and larval fish communities during mid-
634 summer in Disko Bay, West Greenland, *Journal of Plankton Research*, 37, 554–570, 2015.

635 Murphy, J. and Riley, J. P.: A modified single solution method for the determination of phosphate in natural waters, *Analytica chimica acta*,
636 27, 31–36, 1962.

637 Myers, P. G. and Ribergaard, M. H.: Warming of the polar water layer in Disko Bay and potential impact on Jakobshavn Isbrae, *Journal of
638 Physical Oceanography*, 43, 2629–2640, 2013.

639 Patro, R., Duggal, G., Love, M. I., Irizarry, R. A., and Kingsford, C.: Salmon provides fast and bias-aware quantification of transcript
640 expression, *Nature methods*, 14, 417–419, 2017.

641 Redfield, A. C.: On the proportions of organic derivatives in sea water and their relation to the composition of plankton (Vol. 1). Liverpool:
642 university press of liverpool, 1934.

643 Reeder, C. F., Stoltenberg, I., Javidpour, J., and Löscher, C. R.: Salinity as a key control on the diazotrophic community composition in the
644 Baltic Sea, *Ocean Science Discussions*, 2021, 1–30, 2021.

645 Rees, A. P., Gilbert, J. A., and Kelly-Gerrey, B. A.: Nitrogen fixation in the western English Channel (NE Atlantic ocean), *Marine Ecology
646 Progress Series*, 374, 7–12, 2009.

647 Rysgaard, S., Boone, W., Carlson, D., Sejr, M., Bendtsen, J., Juul-Pedersen, T., Lund, H., Meire, L., and Mortensen, J.: An updated view on
648 water masses on the pan-west Greenland continental shelf and their link to proglacial fjords, *Journal of Geophysical Research: Oceans*,
649 125, e2019JC015 564, 2020.

650 Schiøtt, S.: The Marine Ecosystem of Ilulissat Icefjord, Greenland, Ph.D. thesis, Department of Biology, Aarhus University, Denmark, 2023.

651 Schlitzer, R.: Ocean data view, 2022.

652 Schwarcz, C. R., Wilson, S. T., Caffin, M., Stancheva, R., Li, Q., Turk-Kubo, K. A., White, A. E., Karl, D. M., Zehr, J. P., and Steward, G. F.:

653 Overlooked and widespread pennate diatom-diazotroph symbioses in the sea, *Nature communications*, 13, 799, 2022.

654 Shao, Z., Xu, Y., Wang, H., Luo, W., Wang, L., Huang, Y., Agawin, N. S. R., Ahmed, A., Benavides, M., Bentzon-Tilia, M., et al.: Global
655 oceanic diazotroph database version 2 and elevated estimate of global N₂ fixation, *Earth System Science Data*, 15, 2023.

656 Sherwood, O. A., Davin, S. H., Lehmann, N., Buchwald, C., Edinger, E. N., Lehmann, M. F., and Kienast, M.: Stable isotope ratios in
657 seawater nitrate reflect the influence of Pacific water along the northwest Atlantic margin, *Biogeosciences*, 18, 4491–4510, 2021.

658 Shiozaki, T., Bombar, D., Riemann, L., Hashihama, F., Takeda, S., Yamaguchi, T., Ehama, M., Hamasaki, K., and Furuya, K.: Basin scale
659 variability of active diazotrophs and nitrogen fixation in the North Pacific, from the tropics to the subarctic Bering Sea, *Global Biogeochemical Cycles*, 31, 996–1009, 2017.

660 Shiozaki, T., Fujiwara, A., Ijichi, M., Harada, N., Nishino, S., Nishi, S., Nagata, T., and Hamasaki, K.: Diazotroph community structure and
661 the role of nitrogen fixation in the nitrogen cycle in the Chukchi Sea (western Arctic Ocean), *Limnology and Oceanography*, 63, 2191–
662 2205, 2018.

663 Shiozaki, T., Fujiwara, A., Inomura, K., Hirose, Y., Hashihama, F., and Harada, N.: Biological nitrogen fixation detected under Antarctic sea
664 ice, *Nature geoscience*, 13, 729–732, 2020.

665 Shiozaki, T., Nishimura, Y., Yoshizawa, S., Takami, H., Hamasaki, K., Fujiwara, A., Nishino, S., and Harada, N.: Distribution and survival
666 strategies of endemic and cosmopolitan diazotrophs in the Arctic Ocean, *The ISME journal*, 17, 1340–1350, 2023.

667 Sigman, D. M., DiFiore, P. J., Hain, M. P., Deutsch, C., Wang, Y., Karl, D. M., Knapp, A. N., Lehmann, M. F., and Pantoja, S.: The dual
668 isotopes of deep nitrate as a constraint on the cycle and budget of oceanic fixed nitrogen, *Deep Sea Research Part I: Oceanographic
669 Research Papers*, 56, 1419–1439, 2009.

670 Sipler, R. E., Gong, D., Baer, S. E., Sanderson, M. P., Roberts, Q. N., Mulholland, M. R., and Bronk, D. A.: Preliminary estimates of the
671 contribution of Arctic nitrogen fixation to the global nitrogen budget, *Limnology and Oceanography Letters*, 2, 159–166, 2017.

672 Slawyk, G., Collos, Y., and Auclair, J.-C.: The use of the ¹³C and ¹⁵N isotopes for the simultaneous measurement of carbon and nitrogen
673 turnover rates in marine phytoplankton 1, *Limnology and Oceanography*, 22, 925–932, 1977.

674 Sohm, J. A., Webb, E. A., and Capone, D. G.: Emerging patterns of marine nitrogen fixation, *Nature Reviews Microbiology*, 9, 499–508,
675 2011.

676 Sterner, R. W., & Elser, J. J. *Ecological stoichiometry: the biology of elements from molecules to the biosphere*. In *Ecological stoichiometry*.
677 Princeton university press, 2017.

678 Tang, W., Wang, S., Fonseca-Batista, D., Dehairs, F., Gifford, S., Gonzalez, A. G., Gallinari, M., Planquette, H., Sarthou, G., and Cassar, N.:
679 Revisiting the distribution of oceanic N₂ fixation and estimating diazotrophic contribution to marine production, *Nature communications*,
680 10, 831, 2019.

681 Tremblay, J.-É. and Gagnon, J.: The effects of irradiance and nutrient supply on the productivity of Arctic waters: a perspective on climate
682 change, in: *Influence of climate change on the changing arctic and sub-arctic conditions*, pp. 73–93, Springer, 2009.

683 Turk, K. A., Rees, A. P., Zehr, J. P., Pereira, N., Swift, P., Shelley, R., Lohan, M., Woodward, E. M. S., and Gilbert, J.: Nitrogen fixation and
684 nitrogenase (*nifH*) expression in tropical waters of the eastern North Atlantic, *The ISME journal*, 5, 1201–1212, 2011.

685 Turk-Kubo, K. A., Frank, I. E., Hogan, M. E., Desnues, A., Bonnet, S., and Zehr, J. P.: Diazotroph community succession during the VAHINE
686 mesocosm experiment (New Caledonia lagoon), *Biogeosciences*, 12, 7435–7452, 2015.

687 Von Friesen, L. W. and Riemann, L.: Nitrogen fixation in a changing Arctic Ocean: an overlooked source of nitrogen?, *Frontiers in Microbiology*,
688 11, 596 426, 2020.

689

690 Wang, S., Bailey, D., Lindsay, K., Moore, J., and Holland, M.: Impact of sea ice on the marine iron cycle and phytoplankton productivity,
691 Biogeosciences, 11, 4713–4731, 2014.

692 Zehr, J. P. and Capone, D. G.: Changing perspectives in marine nitrogen fixation, Science, 368, eaay9514, 2020.